Design and Development of Water-splitting Electrocatalysts Based on Conjugated Triazine Frameworks

Boying Zhang[a], Phathutshedzo Khangale[a], Xinying Liu[b],*

[a] Department of Chemical Engineering, University of Johannesburg
[b] Institute for Development of Energy for African Sustainability, University of South Africa
 liux@unisa.ac.za

Covalent triazine frameworks (CTFs) with rich nitrogen atoms and permanent porosity have been widely used in the field of opto/electronics as supports. In this study, two CTFs with different pore sizes (single pore and heteropore) were synthesized, after which Cu^{2+}, Co^{2+}, Ni^{2+}, Pd^{2+}, Pt^{2+}, and the corresponding metal cluster were introduced into the CTFs as catalytic active sites through the confinement effect of the pores. Among a series of CTFs-based electrocatalysts, DCP-CTF-Pt^{2+} displays an outstanding electrocatalytic performance with an overpotential of 46 mV and a Tafel slope of 30.2 mV dec^{-1}. Catalytic kinetics analysis indicates that electrocatalytic performance is closely relevant to hierarchical pore and metal size.

1. Introduction

In the field of clean energy, hydrogen energy is regarded to be one of the most important clean energies of the future. The primary technologies for hydrogen production include thermal and electrolysis of water methods, with the former relying on fossil fuels and chemical feedstocks. Hydrogen production from fossil energy sources, such as water gas and natural gas reforming, has been implemented in industrial settings with relatively mature technology. However, the energy output exceeds the input. If this process is utilized for hydrogen power generation, the energy conversion efficiency would be suboptimal and the economic feasibility would be compromised. Therefore, hydrogen production from conventional energy sources is not an optimal technology for producing hydrogen. Hydrogen production from chemical feedstocks primarily encompasses alcohol cracking and reforming processes, including methanol steam reforming for hydrogen generation. Electrocatalytic water splitting is a promising technology for hydrogen production, in comparison to thermochemical method. At present, platinum-based materials are the optimal electrocatalyst for hydrogen evolution reaction (HER). However, noble metals are scarce and expensive, which limits the development of electrocatalytic for HER. Therefore, it is important to develop high-activity, cost-effective electrocatalysts for commercial-scale water electrolysis for hydrogen production.

According to the synergistic mechanism, the assembly of the second active component on the original support material has been widely developed as high-performance catalysts. Porous carbon materials have been applied as catalytic carriers, Covalent triazine frameworks (CTFs) containing triazine moieties, are class of porous organic polymers with conjugated skeleton. Using CTFs as the catalyst support shows increasing potential in electrocatalysts, as: (a) CTFs with a conjugated aromatic skeleton are facilitated to electronic migration; (b) CTFs show good physical/chemical stability; (c) numerous heteroatoms allow CTFs to interact with metallic species. In the second active species, metal clusters and metal single atoms are considered the best candidates for integration with CTFs for electrocatalysis. (Yi et al., 2019) prepared a porous porphyrinic triazine-based framework with anchoring Co–N_4 moiety. With well-dispersed single-atom Co and a hierarchical porous structure, the electrocatalyst exhibited excellent performance for both the oxygen reduction reaction (ORR) and HER. (Qiao et al., 2019) used high crystalline CTFs as supports to load MoS_2 for HER. The CTF@MoS_2 displayed outstanding catalytic activity, with an overpotential of 93 mV. (Ju et al, 2020) proposed a method to enhance HER performance by means of uniformly loading Ru on the triazine-ring-doped carbon carrier.

In this study, two building blocks with different geometry were selected to synthesize CTFs with different pore structures. Two CTFs were modified by metal clusters or metal ions (Cu, Ni, Co, Pd and Pt). The metal cluster or metal ion modified CTFs (named CTF-MC and CTFs-M^{2+}) were evaluated as electrocatalysts for HER (Figure 1). It was found that the catalytic activity was impacted by porosity, metal species and size of the metal particle.
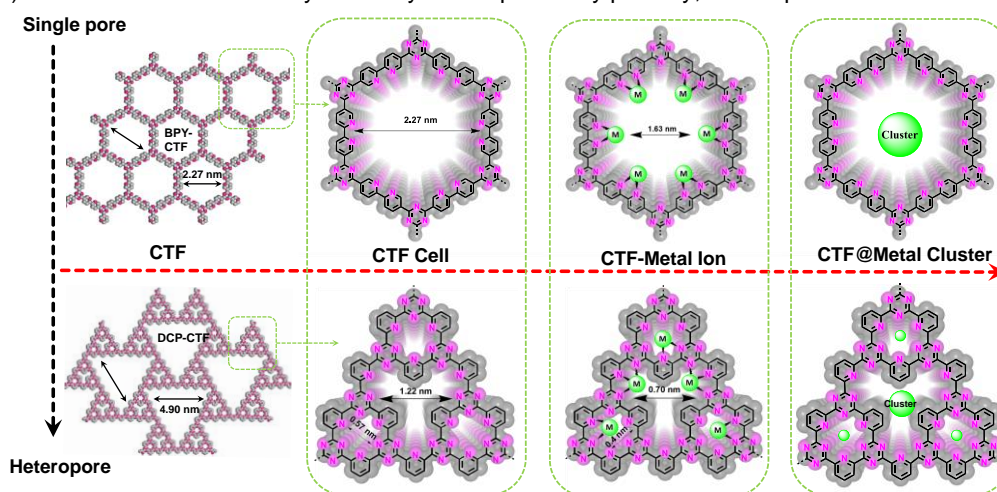

Figure 1. Schematic demonstrations of as-synthesized CTFs, metal ions and metal clusters modified using CTFs (M represents Cu, Co, Ni, Pd and Pt).

2. Characterization

The samples were prepared using a tubular furnace provided by Thermal Fish Scientific. The nitrogen adsorption/desorption measurements were conducted using the Quantachrome Autosorb apparatus at a temperature of 77 K. The electrochemical measurements were conducted using a Zennium Pro electrochemical workstation equipped with a three-electrode system. The three-electrode configuration consisted of a glassy carbon electrode (φ=4 mm) coated with catalyst as the working electrode, a carbon rod as the counter electrode, and an Ag/AgCl (sat. KCl) reference electrode.

3. Results and discussion

The ionthermal method was used to synthesize single-pore BPY-CTF and heterpore DCP-CTF (Figure 2). As an example: BPT-CTF, 5,5'-Dicyano-2,2'-bipyridine (BPY) and zinc chloride were placed in a Pyrex tube and protected by a nitrogen atmosphere. The Pyrex tube was evacuated, sealed and heated to 400 °C for 10 h, and then heated at 600 °C for 10 h. The black powder was obtained after removing the zinc chloride.
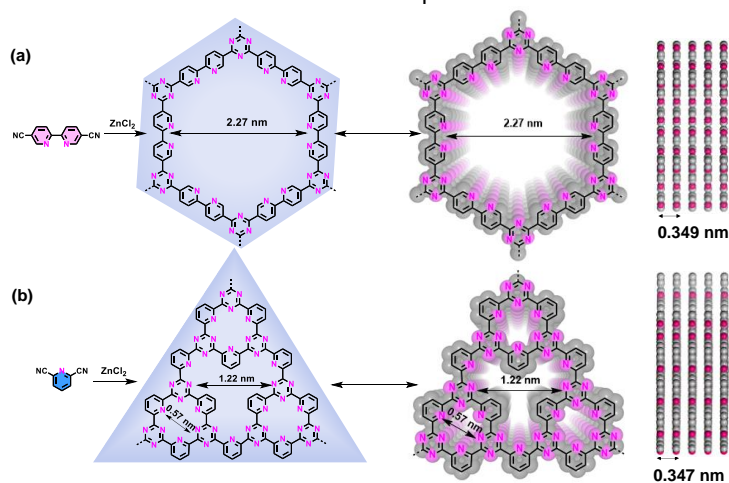

Figure 2 Schematic of the synthesis of (a) BPY-CTF and (b) DCP-CTF, and models of CTFs.

Nitrogen adsorption measurement is used to analyse the permanent porosity of CTFs, CTF-MC and CTFs-M^{2+}. The Brunauer-Emmett-Teller (BET) surface area of BPY-CTF and DCP-CTF was calculated according to nitrogen adsorption/desorption isotherms and was recorded as 2260 and 2230 m^2 g^{-1}, respectively (Figure 3a and b). The pore size distribution calculated using QS-DTF shows that there are some ultrafine pores and mesoporous pores in BPY-CTF (Figure 4a). This may be due to the recombination of carbon atoms caused by the high reaction temperature used. In DCP-CTF (Figure 4b), the pore size distribution is about 1–2 nm and 2–4 nm. These ultra-micropores, micropores and mesoporous pores may provide pathways for transporting reactants and products. After being modified by a metal cluster or metal ion, the isotherms of CTF-MC and CTFs-M^{2+} remained type I isotherms, while the BET of CTF-MC and CTFs-M^{2+} decreased. This indicates that guest molecules are introduced into the channel of CTFs.
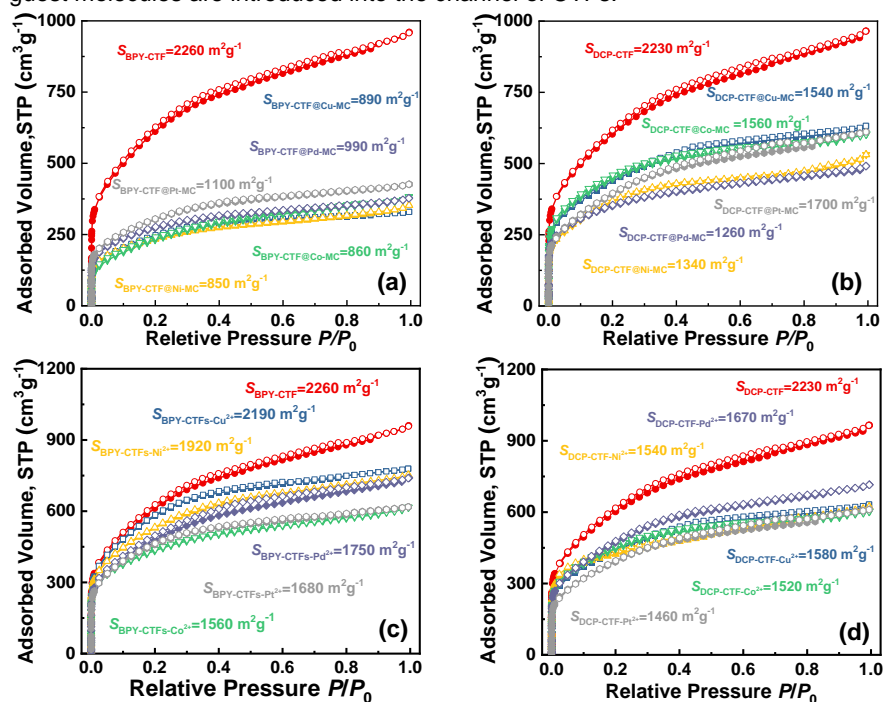

Figure 3. N_2 adsorption/desorption isotherms of BPY-CTF, DCP-CTF, BPY-CTF-MC, DCP-CTF-MC, BPY-CTF-M^{2+} and DCP-CTF-M^{2+}.
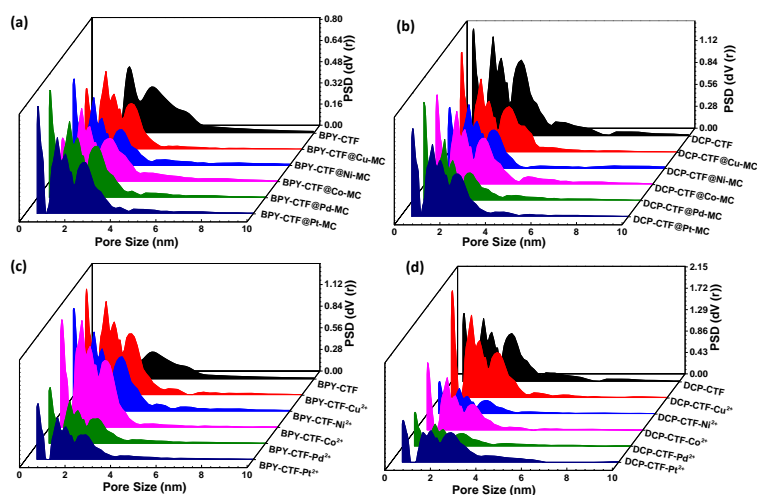

Figure 4. Pore size distribution profiles calculated using QS-DTF for (a) BPY-CTF@MC, (b) DCP-CTF@MC, (c) BPY-CTF-M^{2+} and DCP-CTF-M^{2+}.

Electrochemical measurements were performed in a three-electrode system, with a glassy carbon electrode, Ag/AgCl and a carbon rod used as the working electrode, reference electrode and counter electrode, respectively. Linear sweep voltammetry (LSV) was used to evaluate the overpotential of the electrocatalysts (Figure 5a and d). The overpotential of DCP-CTF was shown to be 155 mV, which is smaller than that of BPY-CTF (355 mV). This may be due to the heteropore structure of DCP-CTF that boosts the mass transfer process. After a metal cluster was integrated into BPY-CTF (Figure 5a), the overpotential of 470, 234, 213, 109 and 117 mV were obtained for BPY-CTF@Cu-MC, BPY-CTF@Co-MC, BPY-CTF@Ni-MC, BPY-CTF@Pd-MC and BPY-CTF@Pt-MC. The overpotential of DCP-CTF@Cu-MC, DCP-CTF@Co-MC, DCP-CTF@Ni-MC, DCP-CTF@Pd-MC and DCP-CTF@Pt-MC was 397, 181, 176, 71, and 60 mV (Figure 5d). These results indicate that metal species have a significant effect on HER performance.

The Tafel slope was applied to investigate catalytic kinetics. (The lower the slope, the faster the electrocatalytic kinetics.) Relative to the Tafel slope of BPY-CTF and DCP-CTF, the slope of the composite decreased, indicating that the catalytic kinetics accelerated (Figure 5b and e). In addition, the reduction in the charge transfer resistance indicates that the composite material has a faster electron transfer efficiency at the interface of the electrode/electrolyte (Figure 5c and f).
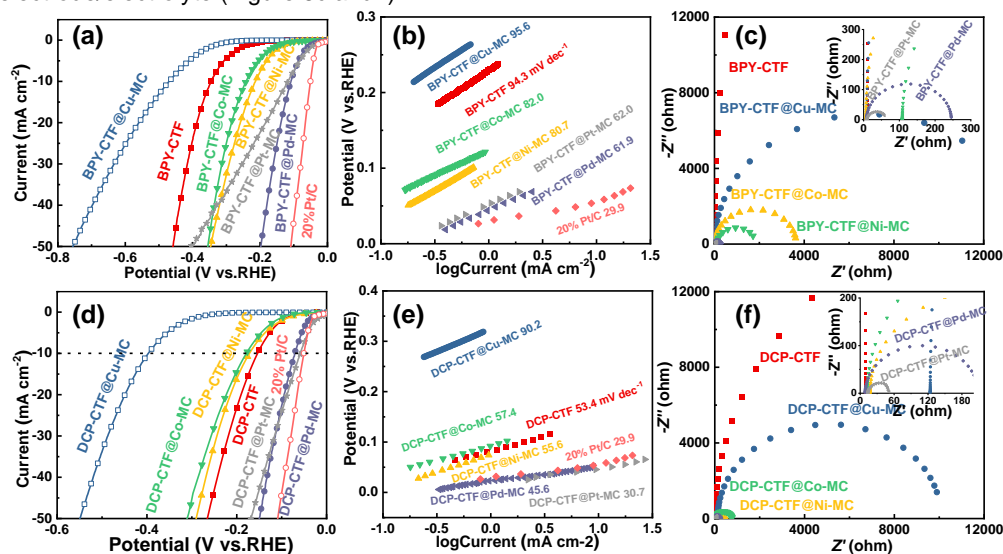

Figure 5. Electrochemical measurements. Linear sweep voltammetry curves of (a) BPY-CTF and BPY-CTF-MC, and (d) DCP-CTF and DCP-CTF-MC. Tafel slope of (b) BPY-CTF and BPY-CTF-MC, and (e) DCP-CTF and DCP-CTF-MC. Nyquist plots of (c) BPY-CTF and BPY-CTF-MC, and (f) DCP-CTF and DCP-CTF-MC.

As shown in Figure 6a and d, CTFs-M^{2+} show a dramatic increase in cathode current. Compared to CTFs-MC, CTFs-M^{2+} exhibit more effective electrocatalytic activity. Surprisingly, DCP-CTF-Pt^{2+} displays an outstanding overpotential of 46 mV, which exceeds that of 20% Pt/C. In CTFs, CTF-MC and CTF-MC^{2+}, DCP-CTF-Pt^{2+} exhibits the smallest Tafel slope of 30.2 mV dec^{-1}. The electrocatalytic mechanism of DCP-CTF-Pt^{2+} is Volmer–Tafel. Nyquist plots were used to investigate the charge transfer resistance (R_{ct}). CTF-M^{2+} show much smaller resistance relative to CTF-MC, indicating fast electron transfer in the interface between electrode and electrolyte. As shown in Figure 6i, cyclic voltammetry was done to test the stability of DCP-CTF-Pt^{2+}. The results show that the overpotential of DCP-CTF-Pt^{2+} barely changed after 3000 cycles. The exchange current density of DCP-CTF-Pt^{2+} is 0.41 mA cm^{-2}, which is comparable to 20% Pt/C (Figure 6h). These results indicate that CTF acts as a conductive carrier, and provides anchoring sites for metal ions, which greatly improves metal utilization.

It was found that DCP-CTF-based electrocatalysts show excellent catalytic activity when comparing BPY-CTF and DCP-CTF-based catalysts (Table 1). This may be related to the following: (a) hierarchical porous materials improve the efficiency of electrolyte diffusion and gas diffusion in the electrocatalytic process. (b) DCP-CTF has abundant porosity, which means exposure of more active sites; (c) DCP-CTF possesses an abundance of nitrogen atoms on which to anchor the metal ions, thus achieving atomic-level dispersion of the metals.
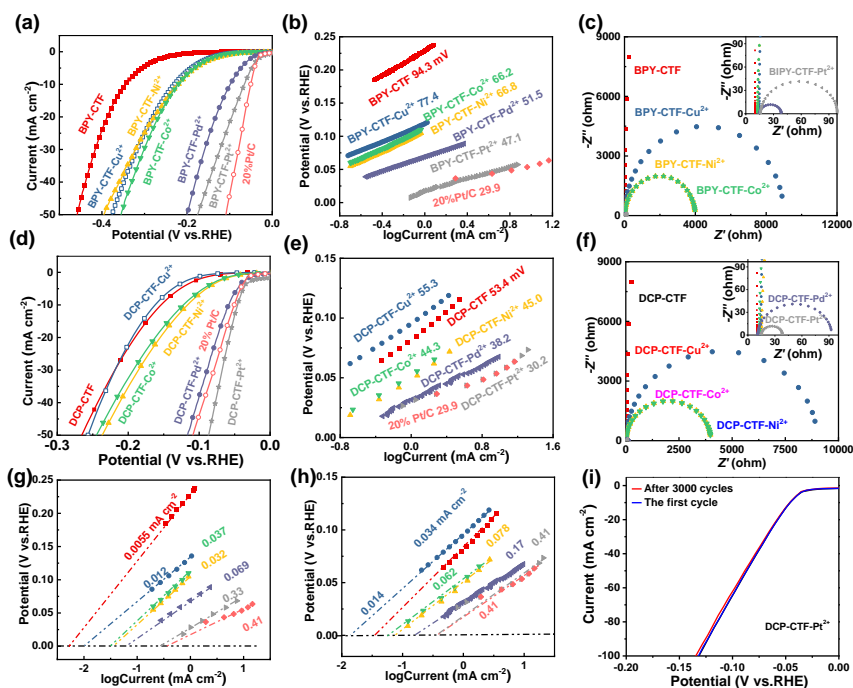
Figure 6. Electrochemical measurements. Linear sweep voltammetry curves of (a) BPY-CTF and BPY-CTF-M^{2+}, and (d) DCP-CTF and DCP-CTF-M^{2+}. Tafel slope of (b) BPY-CTF and BPY-CTF-M^{2+}, and (e) DCP-CTF and DCP-CTF-M^{2+}. Nyquist plots of (c) BPY-CTF and BPY-CTF-M^{2+}, and (f) DCP-CTF and DCP-CTF-M^{2+}. Exchange current density of (g) BPY-CTF and BPY-CTF-M^{2+}, and (h) DCP-CTF and DCP-CTF-M^{2+}. (i) Stability test of DCP-CTF-Pt^{2+} after 3000-cycle.

Table 1 Comparison of electrocatalytic properties of BPY-CTF, DCP-CTF, BPY-CTF-M^{2+}, DCP-CTF-M^{2+}, BPY-CTF@MC and DCP-CTF@MC.

Catalyst	Overpotential/mV @10mA cm^{-2} versus RHE	Tafel slope (mV dec^{-1})	Exchange current density (mA cm^{-2})	C_{dl} (mF cm^{-2})
BPY-CTF	345	94.3	0.0055	1.50
BPY-CTF-Cu^{2+}	230	77.4	0.0120	1.52
BPY-CTF-Co^{2+}	221	66.2	0.0320	1.82
BPY-CTF-Ni^{2+}	220	66.8	0.0370	1.83
BPY-CTF-Pd^{2+}	99	51.5	0.0690	8.68
BPY-CTF-Pt^{2+}	66	47.1	0.3300	11.10
BPY-CTF@Cu-MC	470	95.6	0.0020	0.08
BPY-CTF@Co-MC	234	82.0	0.0160	1.51
BPY-CTF@Ni-MC	213	80.7	0.0430	1.93
BPY-CTF@Pd-MC	109	61.9	0.1900	6.54
BPY-CTF@Pt-MC	117	62.0	0.1700	6.20
DCP-CTF	155	53.4	0.0340	3.77
DCP-CTF-Cu^{2+}	162	55.3	0.0140	3.20
DCP-CTF-Co^{2+}	121	44.3	0.0620	4.77
DCP-CTF-Ni^{2+}	121	45.0	0.0780	4.80
DCP-CTF-Pd^{2+}	58	38.2	0.1720	12.40
DCP-CTF-Pt^{2+}	46	30.2	0.4100	16.00
DCP-CTF@Cu-MC	397	90.2	0.0050	0.80
DCP-CTF@Co-MC	181	57.4	0.0400	1.98
DCP-CTF@Ni-MC	176	55.6	0.1000	2.20
DCP-CTF@Pd-MC	71	45.6	0.2200	9.60
DCP-CTF@Pt-MC	60	30.7	0.4000	12.05

4. Conclusions

The design of two distinct CTFs with diverse porous structures was followed by their modification through the incorporation of metal clusters or metal ions. The CTFs-MC and CTFs-M^{2+} electrocatalysts obtained were assessed for their suitability in HER. The DCP-CTF series of catalysts have demonstrated exceptional catalytic performance. A heteroporous structure is proposed to optimize transfer rates, encompassing electrolyte diffusion, gas diffusion, and electron transfer, which are often challenging to observe in single-porous materials. Moreover, the abundant porosity of heteroporous frameworks exposes a greater number of accessible active sites. DCP-CTF exhibits a higher nitrogen content in comparison to BPY-CTF, and DCP-CTF-Pt^{2+} demonstrates exceptional electrocatalytic performance with an overpotential of 46 mV and a Tafel slope of 30.2 mV dec^{-1}. It has been demonstrated in this investigation that hierarchical pores confer benefits for gas diffusion, electrolyte diffusion, and electron transfer; abundant porosity enhances the utilization rate of active sites; and the metal size effect plays a pivotal role in HER.

References

Ju Q., Ma, R., Pei, Y., Guo, B., Li, Z., Liu, Q., Thomas, T., Yang, M., Hutchings, G. J., Wang, J., 2020, Ruthenium triazine composite: A good match for increasing hydrogen evolution activity through contact electrification. Advanced Energy Materials, 10, 2000067.

Li Y. , Lai, C., Liu, S., Fu, Y., Qin, L., Xu, M., Ma, D., Zhou, X., Xu, F., Liu, H., Li, L., Sun, Q., Wang, N., 2023, Metallic active-site engineering: A bridge between covalent triazine frameworks and high-performance catalysts. Journal of Materials Chemistry A, 11, 2070–2091.

Qiao S. , Zhang, B., Li, Q., Li, Z., Wang, W., Zhao, J., Zhang, X., Hu, Y., 2019, Pore surface engineering of covalent triazine frameworks@MoS$_2$ electrocatalyst for the hydrogen evolution reaction. ChemSuchem, 12, 5032–5040.

Yan Y., He, T., Zhao, B., Qi, K., Liu, H., Xia, B. Y., 2018, Metal/covalent–organic frameworks-based electrocatalysts for water splitting. Journal of Materials Chemistry A, 6, 15905–15926.

Yi J.D., Xu, R., Chai, G-L., Zhang, T., Zang, K., Nan, B., Lin, H., Liang, Y-L., Lv, J., Luo, J., Si, R., Huang, Y-B., Cao, R., 2019, Cobalt single-atoms anchored on porphyrinic triazine-based frameworks as bifunctional electrocatalysts for oxygen reduction and hydrogen evolution reactions. Journal of Materials Chemistry A, 7, 1252–1259.